A Chromium-thiolate complex undergoing C-S bond cleavage

Kaiji Shen,[a] Marcello Gennari,[a] Christian Philouze, Ajdin Velić,[b] Serhiy Demeshko,[b]
Franc Meyer,[b] Carole Duboc[a,*]

[a] *Univ. Grenoble Alpes, CNRS UMR 5250, DCM, F-38000 Grenoble, France*
[b] *University of Göttingen, Institute of Inorganic Chemistry, Tammannstrasse 4, D- 37077 Göttingen, Germany*

corresponding author: carole.duboc@univ-grenoble-alpes.fr

Abstract

The cleavage of C-S bonds represents a crucial step in the fossil fuel refinement to remove organosulfur impurities. Efforts are required to identify alternatives that can replace the energy-intensive hydrodesulfurization process currently in use. In this context, we have developed a series of bis-thiolate Cr^{III} complexes supported by the L^{2-} ligand (L^{2-} = 2,2'-bipyridine-6,6'-diyl(bis(1,1-diphenylethanethiolate), one of them displaying desulfurization of one thiolate of the ligand under reducing and acidic conditions at ambient temperature and atmospheric pressure. While only 5-coordinated complexes were previously isolated by reaction of L^{2-} with 3-d metal M^{III} ions, both 5- and 6-coordinated mononuclear complexes have been obtained in the case of Cr^{III}, viz., $[Cr^{III}LCl]$, $[Cr^{III}LCl_2]^-$, and $[Cr^{III}LCl(CH_3CN)]$. The investigation of the reactivity of $[Cr^{III}LCl(CH_3CN)]$ under reducing conditions led to a dinuclear $[Cr^{III}_2L_2(\mu\text{-}Cl)(\mu\text{-}OH)]$ compound and, in the presence of protons, to the mononuclear Cr^{III} complex $[Cr^{III}(L^{N2S})_2]^+$, where L^{N2S-} is the partially desulfurized form of L^{2-}. A desulfurization mechanism has been proposed involving the release of H_2S, as evidenced experimentally.

Introduction

Cleaving a C-S bond remains a major chemical challenge in the context of hydrodesulfurization (HDS) in fossil fuels. HDS is a crucial industrial catalytic process aimed at producing cleaner hydrocarbon products by eliminating organosulfur impurities from oil as H_2S. This process relies on a Mo-sulfide catalyst containing cobalt and operates under high pressure (160-600 psi pressure of H_2) and high temperature (300-450°C).[1-4] Developing a desulfurization pathway with reduced energy consumption becomes urgent to foster a sustainable industrial paradigm shift. In this context, exploring transition metal ions and their reactivity towards sulfur-based organic substrates emerges as an attractive alternative.[5]

Diverse hydrodesulfurization approaches using different transition metal ions have been reported in the literature, [6-19] with only a few working under catalytic conditions.[20-24] In the main cases, C-S bond cleavage occurs after sulfur coordination to the metal ion and involves metal insertion, resulting in hydrosulfide metal complexes. Examples of complete desulfurization with molecular complexes involving decoordination of the resulting sulfur moiety, are relatively uncommon,[6, 20, 25] and generally require prolonged exposure to irradiation or UV light, or high temperature or pressure of H_2 over a long period.

In this study, we have explored a series of bis-thiolate Cr^{III} complexes bearing the ligand L^{2-} (L^{2-} = 2,2'-bipyridine-6,6'-diyl(bis(1,1-diphenylethanethiolate),[26] which was successfully employed in the synthesis of 3d-metal complexes for different purposes in the domain of bio-inspired chemistry,

particularly in relation to (electro)catalytic reduction processes.[27-28] Five new thiolate-supported Cr^{III} complexes, including the 6-coordinated $[Cp_2Co][Cr^{III}LCl_2]$ and $[Cr^{III}LCl(CH_3CN)]$, and 5-coordinated $[Cr^{III}LCl]$ (Scheme 1) were isolated and characterized. Interestingly, $[Cp_2Co][Cr^{III}LCl_2]$ and $[Cr^{III}LCl(CH_3CN)]$ are the first examples of 6-coordinated complexes supported by L^{2-} with M^{III} ions, since only 5-coordinated complexes were previously isolated (M= Ni, Co, Fe, Mn). [29-32] Unexpectedly, we evidenced that when $[Cr^{III}LCl(CH_3CN)]$ is exposed to reducing and acidic conditions, the ligand undergoes desulfurization, conditions that are pertinent to the hydrogen evolution reaction (HER). In light of this, we subsequently discussed the mechanistic aspects of this reaction to rationalize this observed reactivity.

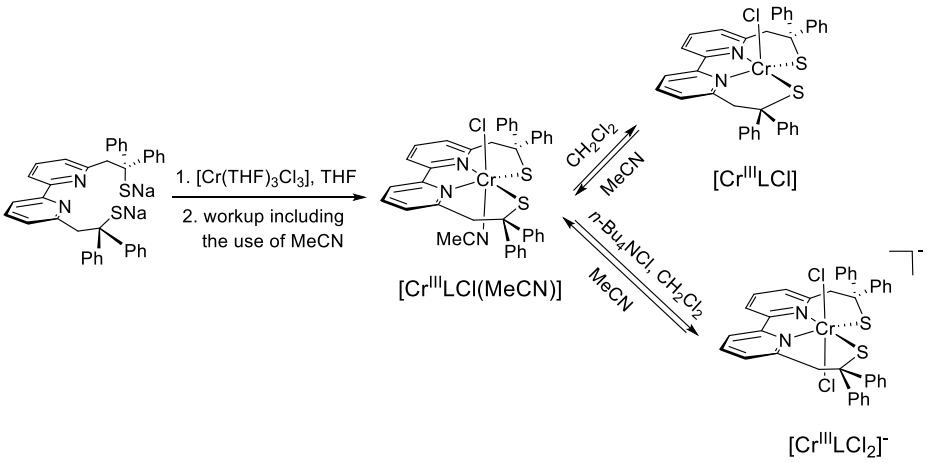

Scheme 1. Chemical paths for synthesizing the complexes $[Cr^{III}LCl]$, $[Cr^{III}LCl(CH_3CN)]$ and $[Cr^{III}LCl_2]^-$.

Results

Synthesis and X-ray structures of a series of mononuclear dithiolate-based Cr^{III} complexes. The $[Cr^{III}LCl(CH_3CN)]$ complex was isolated as a yellow solid by a reaction between L^{2-} and $[Cr^{III}(THF)_3Cl_3]$ in THF and following treatment involving the use of MeCN (Scheme 1). The X-ray diffraction structure of the complex, resolved from single crystals grown by diffusion of CH_3CN into a CH_2Cl_2 solution of the product, reveals a 6-coordinated Cr^{III} complex. When the product is redissolved in CH_2Cl_2 in the absence and presence of an excess of chlorides (*n*-Bu_4NCl or $[CoCp_2]Cl$), the red-purple 5-coordinated complex $[Cr^{III}LCl]$ and the red-orange 6-coordinated complex $[Cp_2Co][Cr^{III}LCl_2]$ were isolated (Scheme 1) and characterized by X-ray diffraction (Fig. 1). Table 1 gives selected bond distances of the three complexes (see SI for more details, Tables S1-S3).

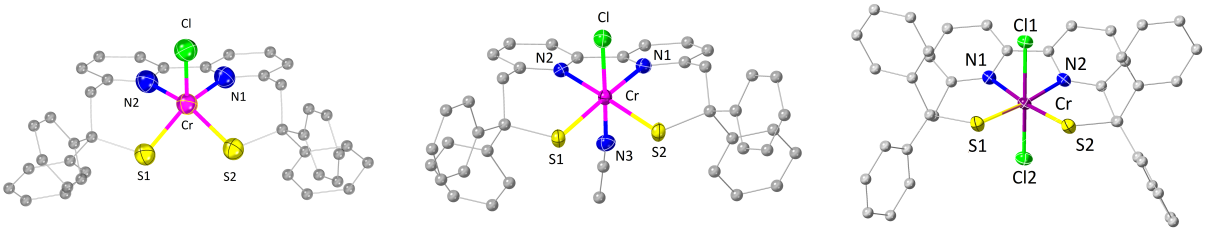

$[Cr^{III}LCl]$ $[Cr^{III}LCl(CH_3CN)]$ $[Cp_2Co][Cr^{III}LCl_2]$

Figure 1. Molecular structures of [Cr^{III}LCl], [Cr^{III}LCl(CH_3CN)], [Cp_2Co][$Cr^{III}LCl_2$] determined by single-crystal X-ray diffraction. The thermal ellipsoids of the metal cores are drawn at a 30% probability level. All hydrogen atoms and solvent molecules are omitted for clarity.

Table 1. Selected bond distances for the [Cr^{III}LCl], [Cr^{III}LCl(CH_3CN)], [Cp_2Co][$Cr^{III}LCl_2$] complexes

[Cr^{III}LCl]		[Cr^{III}LCl(CH_3CN)]		[Cp_2Co][$Cr^{III}LCl_2$]	
Cr−S1	2.283(20)	Cr−S1	2.353(15)	Cr−S1	2.348(04)
Cr−S2	2.291(84)	Cr−S2	2.334(25)	Cr−S2	2.355(22)
Cr−N1	2.063(19)	Cr−N1	2.0928(0)	Cr−N1	2.075(61)
Cr−N2	2.068(66)	Cr−N2	2.077(07)	Cr−N2	2.079(16)
Cr−Cl	2.244(90)	Cr−N3	2.106(43)	Cr−Cl1	2.409(96)
		Cr−Cl	2.328(96)	Cr−Cl2	2.362(19)

In the pentacoordinated [Cr^{III}LCl] complex, the chromium center is in a distorted square planar pyramidal geometry (τ_5 value of 0.058)[33] with the chloride occupying the apical position (d_{Cr-Cl} = 2.244(90) Å) and the N2S2 donor atoms of the L ligand in the equatorial plane. [Cr^{III}LCl] is isostructural to the previously described parent complexes [Fe^{III}LCl] (τ_5 value of 0.328, d_{Fe-Cl} = 2.313 Å)[31] and [Co^{III}LCl] (τ_5 value of 0.360, d_{Co-Cl} = 2.3336(5) Å).[30] The comparison between these three structures evidences that going from Co to Cr, the geometry around the metal ion is less distorted. The distance between the metal ion and the mean N2S2 plane follows the inverse trend, 0.485 Å, 0. 537 Å, and 0.548 Å for the Co, Fe, and Cr complexes, respectively. However, a recent analysis of all the available structures of five-coordinated complexes showed no direct correlation between the τ_5 value and the distance between the metal and the basal plane.[34]

In contrast to all other five-coordinated complexes that have been previously isolated and characterized with L^{2-}, i.e. [M^{III}LX] (M= Co, Fe, Mn; X = Cl, Br, I),[30-32] a sixth ligand, either a solvent molecule or an additional chloride, can coordinate to the Cr^{III} center, leading to six-coordinated mononuclear Cr^{III} complexes, i.e. [Cr^{III}LCl(CH_3CN)] and [Cp_2Co][$Cr^{III}LCl_2$]. This likely reflects the high ligand field stabilization energy for the d^3 Cr^{III} ion in octahedral geometry. As expected, in the dissymmetric [Cr^{III}LCl(CH_3CN)] complex, the Cr^{III} center is displaced towards the chlorido ligand by 0.148 Å, as measured from the mean N2S2 plane towards Cl^-. In contrast, a negligible displacement is observed in the symmetric complex [Cp_2Co][$Cr^{III}LCl_2$], ranging from 0.074 Å to 0.084 Å. Besides, an expected elongation of the Cr-Cl bond(s) compared to [Cr^{III}LCl] is observed in both [Cr^{III}LCl(CH_3CN)] (d_{Cr-Cl} = 2.328(96) Å) and [Cp_2Co][$Cr^{III}LCl_2$] (d_{Cr-Cl} = 2.409(96) Å and 2.362(19) Å).

Characterization of the mononuclear dithiolate-based Cr^{III} complexes. The positive ion ESI mass spectrum of the 5-coordinated [Cr^{III}LCl] complex exhibits the expected peak at m/z = +630.04 for [$Cr^{III}L]^+$, the chloride ligand being lost to generate a positive ion (Fig. S2). The UV-vis spectrum of a dark red solution of [Cr^{III}LCl] in CH_2Cl_2 reveals two intense bands at 440 nm and 530 nm, attributed to charge transfer transitions, and a d-d transition at 725 nm (Fig. 3A).

The magnetic susceptibility of [Cr^{III}LCl], [Cr^{III}LCl(CH_3CN)], and *n*-Bu_4N[$Cr^{III}LCl_2$] was measured between 2 K and 295 K (Fig. 2A and Figs. S6-7). The $\chi_M T$ values at room temperature lie between 1.61 and 1.75 $cm^3mol^{-1}K$ for all three compounds and confirm an S = 3/2 ground state with an expected spin-only value of 1.875 $cm^3mol^{-1}K$. The variable temperature-variable field magnetization measurements reveal a quite small zero-field splitting |D| of ca. 1 cm^{-1} for all compounds. The EPR spectra of [Cr^{III}LCl] recorded both in the solid state and in a CH_2Cl_2 solution display features at low magnetic fields consistent with an S = 3/2 spin state, and their similar patterns show that the five-coordinated geometry around the Cr^{III} ion is retained in CH_2Cl_2 (Fig. 2B).

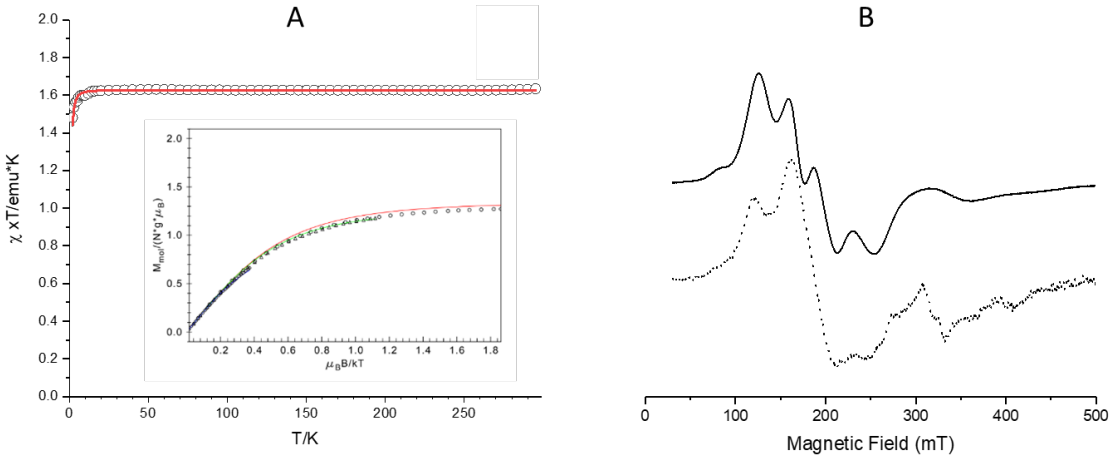

Figure 2. A. $\chi_M T$ versus T plot for [CrLCl]. The inset shows variable temperature-variable field (VTVH) magnetization measurements as M_{mol} versus $\mu_B B/kT$. Solid lines represent the calculated curves fit with parameters g = 1.86 and D = 1.3 cm^{-1}. B. cw X-band EPR spectra of [CrLCl] recorded at 100 K, in solid-state (solid line) and in CH_2Cl_2 solution (dotted line).

To investigate the coordination properties of CH_3CN to the Cr^{III} center in [Cr^{III}LCl] to give [Cr^{III}LCl(CH_3CN)], UV-vis spectra were recorded in a mixture of solvents CH_2Cl_2/CH_3CN with different ratios (1:0 to 1:1) (Fig. 3A). By increasing the amount of CH_3CN, the spectrum drastically evolves: a shift of the band at 530 nm to 500 nm and a decrease in intensity of both features are observed. This agrees with the formation of the hexacoordinated Cr^{III}-MeCN adduct, [Cr^{III}LCl(CH_3CN)], characterized by X-ray diffraction (see above). When the CH_2Cl_2:CH_3CN ratio reaches the value of 1, the adduct starts to precipitate and can be isolated. Interestingly, the process is fully reversible: when crystals of [Cr^{III}LCl(CH_3CN)] are redissolved in CH_2Cl_2, the UV-vis spectrum evidences the formation of [Cr^{III}LCl].

As observed with the addition of CH_3CN, when increasing amounts of *n*-Bu_4NCl are added to a CH_2Cl_2 solution of [Cr^{III}LCl] (from 0 to 200 eq, Fig. 3B), a hypsochromic shift of the two main transitions accompanied by a loss of intensity is observed in the UV-vis spectrum. This agrees with the formation of the hexacoordinated adduct *n*-Bu_4N[$Cr^{III}LCl_2$]. In both octahedral complexes, the coordination of a sixth ligand also leads to the decrease of the d-d transition intensity.

While the positive ion ESI mass spectrum of [Cr^{III}LCl(CH_3CN)] is indistinguishable from that of [Cr^{III}LCl], with a peak at m/z = 630.04 for [$Cr^{III}L]^+$, the negative ion ESI mass spectrum of [$Cr^{III}LCl_2]^-$ shows a peak at 700.13 m/z corresponding to the molecular ion [$Cr^{III}LCl_2]^-$. Both six-coordinated Cr^{III} complexes, [Cr^{III}LCl(CH_3CN)] and [$Cr^{III}LCl_2]^-$, have the expected S=3/2 ground state as attested by the magnetic data and the respective EPR spectra with low-magnetic field features (Figs. S4-S5).

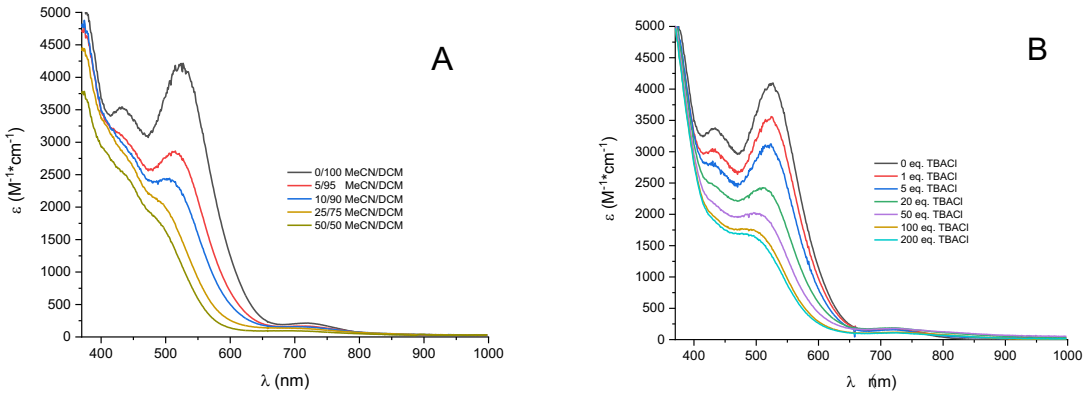

Figure 3. UV−vis spectra of [Cr^{III}LCl] (0.3 mM), A. in a mixture of CH_2Cl_2:CH_3CN with increasing % of MeCN (0 %, 5 %, 10 %, 25 %, and 50 % of MeCN), B. in CH_2Cl_2 (0.25 mM) with various amounts of *n*-Bu_4NCl (0, 1,5, 20, 50, 10, 200 equiv.)

As a preliminary step in the attempt to access Cr^{II} species, the reduction properties of the three mononuclear Cr^{III} complexes have been investigated by cyclic voltammetry (CV). Cathodic scans are shown for 0.1 mM solutions of [Cr^{III}LCl(CH_3CN)] and [$Cr^{III}LCl_2$]$^-$ in MeCN + 0.1 M of electrolyte (*n*-Bu_4NClO_4 and *n*-Bu_4NCl, respectively) in Fig. 4, and for [Cr^{III}LCl] in CH_2Cl_2 + 0.1 M *n*-Bu_4NClO_4 in Fig. S3. All potentials are referred to the Fc^+/Fc redox couple.

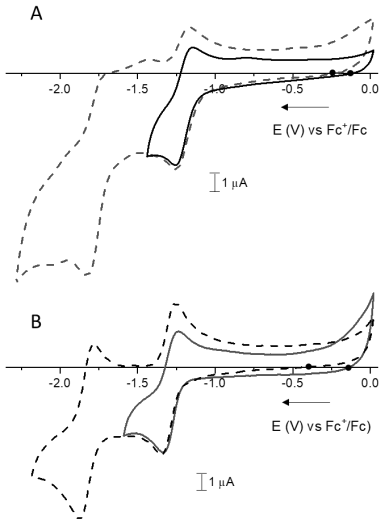

Figure 4. (A) CVs of 0.1 mM solution of [Cr^{III}LCl(CH_3CN)] in MeCN + 0.1 M n-Bu_4NClO_4 recorded on a glassy-carbon working electrode at 100 mV s^{-1}. (B) CVs of 0.1 mM solution of *n*-Bu_4N[$Cr^{III}LCl_2$] in MeCN + 0.1 M n-Bu_4NCl recorded on a glassy-carbon working electrode at 100 mV s^{-1}. Dotted lines for CVs recorded from 0 V to -2.25 V (A) and -2.20 V (B) and bold lines for CVs recorded from 0 V to -1.4 V (A) and – 1.6 V (B).

The three complexes display two successive one-electron reduction processes. The first cathodic peak is observed at $E_{1/2}$ = - 1.20 V for [Cr^{III}LCl(CH_3CN)], $E_{1/2}$ = - 1.29 V for [$Cr^{III}LCl_2$]$^-$, and $E_{1/2}$ = - 1.21 V for [Cr^{III}LCl]. This reduction process is assigned to the reduction of Cr^{III} to Cr^{II}. In [$Cr^{III}LCl_2$]$^-$, the reduction

potential is shifted cathodically by 90 mV compared to [Cr^{III}LCl(CH_3CN)], consistent with the higher donor abilities of a {$N_2S_2Cl_2$} set compared to a {N_2S_2Cl(MeCN)} one. No significant difference is observed between [Cr^{III}LCl(CH_3CN)] and [Cr^{III}LCl], even though such comparison has to be considered with caution due to the different solvents. In the case of [$Cr^{III}LCl_2$]$^-$ and [Cr^{III}LCl], the $Cr^{III/II}$ redox couples are reversible (ΔE_p = 100 mV, ip_c/ip_a = 1.1 and ΔE_p = 120 mV, ip_c/ip_a = 1.1, respectively). This evidences rapid electron transfer and retention of chloride(s) coordination to the Cr^{II} ion at the CV timescale. Concerning [Cr^{III}LCl(CH_3CN)], the Cr^{III}/Cr^{II} redox system at -1.20 V (ΔEp = 110 mV, ip_c/ip_a = 1.2) is accompanied by a secondary weak backward peak at Ep_a = -0.80 V, indicative of partial evolution of the reduced species on the CV timescale.

Regarding the second cathodic redox system, it is observed at Ep_c = -1.83 V (Ep_{a1} = -1.72 V, Ep_{a2} = -1.43V), for [Cr^{III}LCl(CH_3CN)], at Ep_c = -1.87 V (Ep_a = -1.79 V) for [$Cr^{III}LCl_2$]$^-$, and at Ep_c = -1.79 V for [Cr^{III}LCl]. By analogy with other L^{2-}-supported transition metal complexes, it can be assigned to a reduction process primarily localized on the bipyridine unit, with the unpaired electron partly delocalized on the chromium center. [35-37] While this redox system is reversible for [$Cr^{III}LCl_2$]$^-$ (ΔEp = 80 mV, ip_c/ip_a = 1.0), it becomes irreversible in the case of [Cr^{III}LCl(CH_3CN)], highlighting the significant role of the second chloride ligand in stabilizing the doubly reduced product on the CV timescale. In the case of [Cr^{III}LCl], the ~3-fold higher intensity of this second reduction peak compared to that of the first one can be attributed to some extent to the electrocatalytic reduction of CH_2Cl_2 by the doubly-reduced complex, as previously observed in the case of a parent Ni-compound.[35]

Reactivity of [Cr^{III}LCl(CH_3CN)] under reducing conditions. The following work has been performed in CH_3CN to avoid reactivity with CH_2Cl_2 under reducing conditions. With the initial intention of isolating Cr^{II} complexes and based on their redox properties ($E_{1/2}$ = - 1.20 V), we investigated the reaction of [Cr^{III}LCl(CH_3CN)] with Cp_2Co, used as a chemical reducing agent ($E_{1/2}$ = - 1.33 V).[38] During the course of the reaction, a change in the color occurs from yellow to dark green (as evidenced by two bands in the UV-vis spectrum recorded in CH_3CN at 495 nm and 575 n. However, despite numerous attempts, this green species cannot be isolated, consistently evolving into a yellowish species. Crystals suitable for X-ray diffraction analysis have been obtained after the addition of water. The structure revealed the formation of a dinuclear Cr^{III} complex, [$Cr^{III}_2L_2$(μ-Cl)(μ-OH)] (Fig. 5). The formation of this μ-hydroxo dichromium(III) complex under reducing conditions was proposed to occur because of the presence of adventitious water that can reoxidize Cr^{II} into Cr^{III} and provide the hydroxo ligand (Scheme 2). A similar behavior was previously observed in the case of dinuclear Cr complexes with tripodal amino ligands.[39-40]

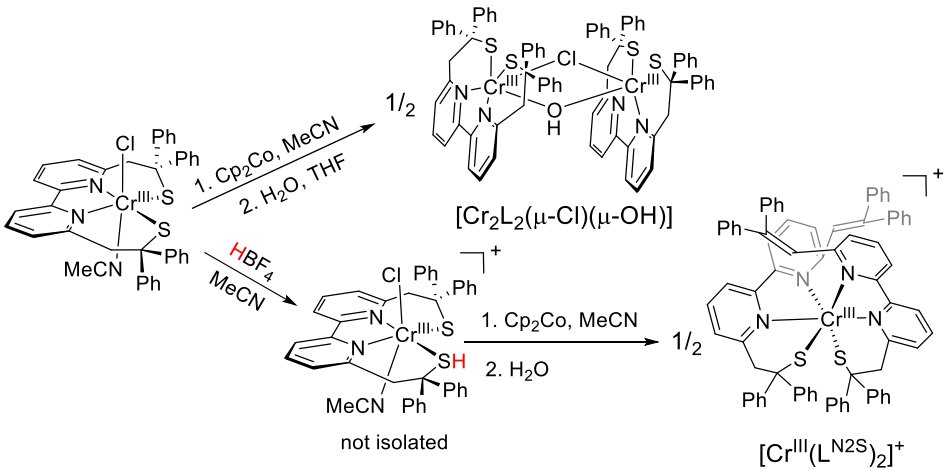

Scheme 2. Synthesis of $[Cr^{III}_2L_2(\mu\text{-}Cl)(\mu\text{-}OH)]$ and $[Cr^{III}(L^{N2S})_2]^+$.

In the structure of $[Cr^{III}_2L_2(\mu\text{-}Cl)(\mu\text{-}OH)]$ (Fig. 5), the two Cr^{III} sites are equivalent with a C_2 symmetry. The two $\{CrL\}^+$ units are bridged by one hydroxo (*trans* to N2) and one chlorido (*trans* to S1) ligand, forming a planar diamond $\{Cr_2O(H)Cl\}$ core with a Cr···Cr distance of 3.383(68) Å. The Cr-O(H) bond (1.9627(101) Å) is shorter than the Cr-Cl one (2.5031(79) Å) and in the expected length range.[41-43] The Cr^{III} ions are in the center of a distorted octahedral geometry with Cr-N and Cr-S bond lengths comparable to those found in $[Cr^{III}LCl(CH_3CN)]$ and $[Cp_2Co][Cr^{III}LCl_2]$ (less than 0.04 Å of difference) (Table 2). Regarding the Cr-Cl bond distance, the bridging mode of the chloride leads to a more significant difference (between 0.09 Å and 0.17 Å longer) compared to terminal Cr-Cl bonds in the previously described Cr^{III} mononuclear complexes.

With the ligand L^{2-}, the only other dinuclear complexes, in which two {ML} units are double bridged with co-ligands, are high-valent Mn^{IV} dimers, specifically $[Mn_2L_2(\mu\text{-}O)(\mu\text{-}OH)]^+$ and $[Mn_2L_2(\mu\text{-}O)_2]$, in which the Mn ion is 6-coordinated.[44] Conversely, at the +III oxidation state, the two {ML} units are only mono-bridged, i.e. $[Mn_2L_2(\mu\text{-}OH)]^+$ and $[Fe_2L_2(\mu\text{-}O)]$.[45-46] This illustrates again the pronounced tendency of d^3 Cr^{III} to adapt an octahedral geometry, in contrast to d^4 Mn^{III} and d^5 Fe^{III}. The Cr-O(H) distance is shorter than those in mono-bridged $[Mn^{III}_2L_2(\mu\text{-}OH)]^+$ (Mn−O(H), 2.034(3) Å and 2.041(3) Å) but comparable with that in the dibridged $[Mn^{IV}_2L_2(\mu\text{-}O)(\mu\text{-}OH)]^+$ (Mn-O(H), 1.959(6) Å).

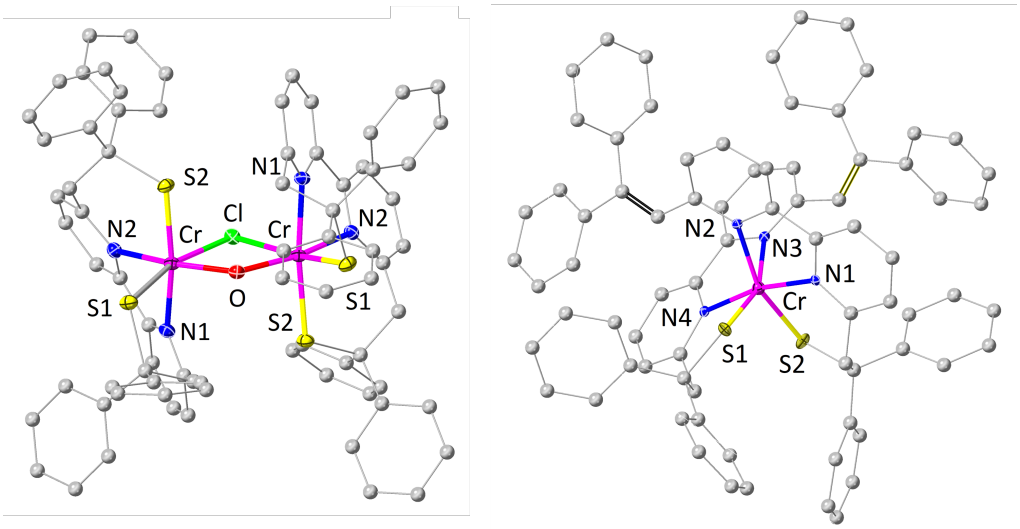

Figure 5. Molecular structures of (left) $[Cr^{III}_2L_2(\mu\text{-}Cl)(\mu\text{-}OH)]$ and (right) $[Cr^{III}(L^{N2S})_2]^+$determined by single-crystal X-ray diffraction. The thermal ellipsoids of the metal cores are drawn at 30% probability level. For clarity, all hydrogen atoms and solvent molecules are omitted.

Table 2. Selected bond distances for the $[Cr^{III}_2L_2(\mu\text{-}Cl)(\mu\text{-}OH)]$ and $[Cr^{III}(L^{N2S})_2]^+$complexes.

$[Cr^{III}_2L_2(\mu\text{-}Cl)(\mu\text{-}OH)]$		$[Cr^{III}(L^{N2S})_2]^+$	
Cr−S1	2.3149(107)	Cr−S1	2.330(49)
Cr−S2	2.3252(36)	Cr−S2	2.342(70)
Cr−N3	2.0785(114)	Cr−N1	2.083(14)
Cr−N4	2.0783(85)	Cr−N2	2.183(08)
Cr−O	1.9627(101)	Cr−N3	2.156(59)
Cr−Cl	2.5031(79)	Cr−N4	2.083(37)
Cr-Cr	3.383(68)		

Attempts were also made to reduce [$Cr^{III}LCl(CH_3CN)$] by Cp_2Co in CH_3CN, in the presence of acid, to better solubilize the initial compound. While Et_3NHBF_4 (pK_a = 18.6 in MeCN)[47] is not strong enough to protonate [$Cr^{III}LCl(CH_3CN)$], it is protonated in the presence of 1 equiv. of $HBF_4{\cdot}Et_2O$ (pK_a = 0.1 in MeCN)[48], as attested by UV-vis spectroscopy (Fig. S1). The [Cr^{III}(LSH)$Cl(CH_3CN)$] complex (LSH being the protonated form of L^{2-} bearing one thiolate and one thiol function), proposed to feature one thiolate and one thiol coordinated to Cr^{III}, can thus be generated *in situ*. After the addition of 1 equiv. of Cp_2Co to [Cr^{III}(LSH)$Cl(CH_3CN)$], crystals of the resulting powder were obtained. The structure still displays a mononuclear Cr^{III} complex (Fig. 4, Table 2), but the metal ion is now found in the center of a distorted octahedral N4S2 environment arising from two tridentate L^{N2S-} ligands (Scheme 2). The L^{N2S-} ligand is generated through the desulfurization of L^{2-}, leading to the loss of the thiol group with the simultaneous formation of a terminal alkene. The Cr-S bonds (2.330(49) Å and 2.342(70) Å) in $[Cr^{III}(L^{N2S})_2]^+$ display similar lengths with respect to those present in the previously described mononuclear octahedral Cr^{III} complexes i.e. [$Cr^{III}LCl(CH_3CN)$] and [Cp_2Co][$Cr^{III}LCl_2$] (between 2.334 Å and 2.355 Å). This observation can be rationalized by the consistent *trans* positioning of the S-donor atoms relative to the N_{bpy}-donor atom in all cases.

Mechanistic considerations regarding the desulfurization process. The chemical reduction of the protonated $[Cr^{III}(LSH)Cl(CH_3CN)]^+$ complex leads to the desulfurization of the ligand accompanied by a rearrangement to generate $[Cr^{III}(L^{N2S})_2]^+$. Under these reductive conditions, two mechanisms to cleave the C-S bond could be envisaged, either through a radical-based cleavage[49-50] or a transitional metal insertion.[51] The latter mechanism can be ruled out since metal insertion should occur under reductive conditions even in the absence of acid. However, only the complex with the intact L^{2-} ligand is observed under these conditions. In the same vein, the LH_2 ligand remains intact in the presence of 1 eq. Cp_2Co.

It has been previously proposed that the presence of an acid is essential in the radical mechanism under reductive conditions since the formation of a thiol triggers the reaction through the generation of the good radical leaving group $HS^{\bullet}$.[50, 52] In the present system, we have demonstrated that thiolate protonation is required to initiate the desulfurization process. Indeed, in the presence of a weak acid (Et_3NHBF_4) that cannot protonate the complex, $[Cr^{III}(L^{N2S})_2]^+$ is not generated under reductive conditions. We also evidenced the absence of H_2 generation during the desulfurization process (before quenching with water), while we observed H_2 production when HBF_4 and Cp_2Co are mixed in the absence of the Cr complex. This rules out the involvement of protonated cobaltocene as observed in previous studies,[53,54] during the desulfurization pathway. Interestingly, after the reaction of $[Cr^{III}(LSH)Cl(CH_3CN)]^+$ with 1 equiv. of Cp_2Co and the subsequent addition of 1 equiv. of $HBF_4{\cdot}Et_2O$ or water, we evidenced the generation of approximately 1 equiv. of H_2S , detected with a fluorophore, the dansyl azide[55] (see Figure S8).

The proposed mechanism for desulfurization is depicted in Scheme 3. The reaction is initiated by the previously mentioned thiolate protonation of [$Cr^{III}LCl(CH_3CN)$] followed by the reduction of the Cr^{III} ion to Cr^{II} in the protonated $[Cr^{III}(LSH)Cl(CH_3CN)]^+$ complex. The generation of a Cr^{II} induces the homolytic cleavage of the C-S bond, leading to the formation of a relatively stable tertiary diphenylalkyl radical $RC(Ph)_2^{\bullet}$, triggering the formation of an alkene function, and a $\{Cr\text{-}SH\}^{2+}$ unit. HS^- is thus released through a concerted mechanism and protonated to generate H_2S after the addition of water or acid, as observed experimentally. Note that even in the presence of an excess of $HBF_4{\cdot}Et_2O$, [$Cr^{III}LCl(CH_3CN)$] can only be mono-protonated, as shown by UV-vis absorption (Fig. S1). For this reason, desulfurization exclusively occurs at one sulfur donor atom of the L^{2-} ligand. The desulfurization process is an effective

route with respect to the metal ion since the conversion of $[Cr^{III}(LSH)Cl(CH_3CN)]^+$ in $[Cr^{III}(L^{N2S})_2]^+$ reaches 29% (with a maximum expected conversion of 50%).

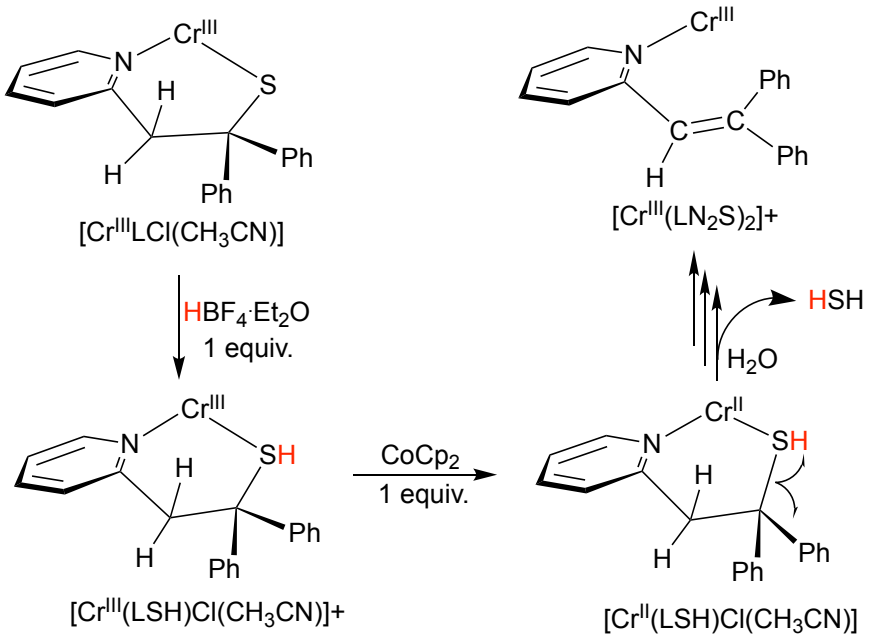

Scheme 3. Simplified mechanism proposed for the desulfurization of $[Cr^{III}LCl(CH_3CN)]$. Only half of the L^{2-} ligand is represented for the sake of simplicity.

Discussion and conclusion

We have synthesized a series of Cr^{III}-based complexes with a bis-thiolate ligand, L^{2-} that has been previously used to synthesize many mononuclear complexes with Zn, Cu, Ni, Co, Fe, and Mn at the +III and/or +II oxidation states.[27-28] All the previous complexes are tetra- or pentacoordinated,[29, 56-58] and we never succeeded in forming a 6-coordinate system, likely because of ligand preorganization effects. Octahedral geometries have been found only in dinuclear complexes with high valent oxidation states in the specific case of Mn.[44,45, 59] The case of 6-coordinated Cr^{III} is thus unique among transition metal ions supported by L^{2-} in the "common" + II and + III oxidation states. This singularity can likely be ascribed to the inherent strong preference of d^3 Cr^{III} to form octahedral complexes, enabling to overcome the "preorganization barrier" of L^{2-}.

Initially, our focus was on evaluating chromium complexes for their (electro)catalytic abilities since 3d-metal-based complexes supported by the bis-thiolate L^{2-} ligand displayed favorable activities in H^+, CO_2, or O_2 reduction.[27] Besides, Machan's group reported an active electrocatalyst for CO_2 reduction with a Cr complex containing a similar ligand in which the S-donor ligands are replaced by O-donor ones, e.g., a bipyridine substituted by two phenols.[60] However, during experiments conducted under reducing conditions, we observed desulfurization of the ligand in the presence of protons with the release of H_2S but no H_2 production. This reactivity poses a notable issue since H^+/e^- conditions are required for achieving the targeted electrocatalytic reduction processes.

In a broader context, stability and durability issues are common among molecular (electro)catalysts involved in reducing small molecules. Identifying the competitive decomposition pathways marks the initial step in solving these problems. Our study reveals desulfurization as a potentially damaging side reaction that occurs under H^+/e^- conditions in metal complexes supported by thiolate ligands. Still, the

use of thiolate-based ligands is inspired by the active sites of several metalloenzymes, which possess a sulfur-rich environment, such as hydrogenases or CO-dehydrogenases. In particular, thiolate ligands have been proposed as beneficial H^+ relays in some of these enzymes and synthetic (electro)catalysts. Therefore, this finding provides valuable insights for designing more advanced thiolate ligands, in which this decomposition pathway should be suppressed, with the aim of developing robust metal-thiolate catalysts for proton-coupled multi-electron reduction processes.

From a different perspective, the present system also stands as a rare example of rapid and complete desulfurization (involving decoordination of the sulfur moiety) occurring at room temperature and pressure and triggered by Cr^{II}. This holds particular significance within the context of fossil fuel refinement by addressing the elimination of organosulfur impurities via a low-energy-consuming process. Ligand design modifications to make the process catalytic, i.e., promoting desulfurization on an external substrate instead of on the ligand itself, are currently underway in the laboratory.

Experimental section.

General. All reagents were used as received. Acetonitrile was distilled over CaH_2 and degassed prior to use. THF was distilled over Na/benzophenone and degassed prior to use. The synthesis of H_2L was reported elsewhere.[26] The synthesis and isolation of all complexes were carried out under argon (in a glove box with less than 5 ppm of O_2). The infrared spectra were recorded on a Thermo Scientific Nicolet iS10 FT-IR spectrometer (equipped with ATR accessory) as neat solids. ^{1}H NMR spectra were recorded on Bruker Avance III 500 MHz spectrometers. The ESI-MS spectra were registered on a Bruker Esquire 3000 Plus or Amazon speed ion trap spectrometer equipped with an electrospray ion source (ESI). The samples were analyzed in positive ionization mode by direct perfusion in the ESI-MS interface (ESI capillary voltage= 2kV, sampling cone voltage= 40 V). The electronic absorption spectra were recorded on a ZEISS MC5601 absorption spectrophotometer in quartz cells (optical path length: 1 cm). Cw-X-band electron paramagnetic resonance (EPR) spectra were recorded with a Bruker EMX, equipped with an Oxford Instruments ESR-900 continuous-flow helium cryostat and an ER-4116 DM Bruker cavity for the 4.5-70 K experiments and equipped with the ER-4192 ST Bruker cavity and an ER-4131 VT for the 100-150 K experiments. Temperature-dependent magnetic susceptibility measurements were carried out with a *Quantum-Design* MPMS3 SQUID magnetometer equipped with a 7 Tesla magnet in the range from 295 to 2.0 K at a magnetic field of 0.5 T. The powdered samples were contained in a gelatin capsule and fixed in a non-magnetic sample holder. Each raw data file for the measured magnetic moment was corrected for the diamagnetic contribution of the sample holder and the gelatin capsule. The molar susceptibility data were corrected for the diamagnetic contribution. Simulation of the experimental magnetic data was performed based on the Hamiltonian $\widehat{H} = g\mu_B\vec{B}\vec{S} + D\left[\hat{S}_z^2 - \frac{1}{3}S(S+1)\right]$ using the *julX_2S* program: E. Bill, Max-Planck Institute for Chemical Energy Conversion, Mülheim/Ruhr, Germany.

X-ray Crystallography. Single-crystal diffraction data for the five Cr^{III} complexes were measured on a Nonius-Bruker 4 circles diffractometer with an APEXII CCD detector and an Incoatec high brilliance micro source with multilayer mirrors to monochromatize the MoKα radiation (λ = 0.71073Å) at 200 K. Eval, Sadabs and Xprep (Nonius-Bruker) were used for cell refinements, integration, absorption correction and data reduction. The OLEX2 program package was used for cell refinements and data reductions. Molecular structures by intrinsic phasing and refined on F^2 by full-matrix least-squares techniques, using the SHELXTL and SHELXL softwares. All non-hydrogen atoms were refined anisotropically, and all hydrogen atoms were placed at their calculated positions.[61] Structures were

deposited with CCDC numbers 2311590 to 2311594 and can be obtained free of charge from The Cambridge Crystallographic Data Centre via www.ccdc.cam.ac.uk/data_request/cif.

Electrochemical measurements. Cyclic voltammetry measurements were carried out in MeCN or CH_2Cl_2 solution (Fisher Sci., HPLC gradient grade), 0.1 M Bu_4NClO_4 (Sigma-Aldrich, for electrochemical analysis ≥99%, used as received), under argon (cyclic voltammetry, CV) atmosphere at 20 °C using a Metrohm-Autolab potentiostat/galvanostat. A standard three-electrode electrochemical cell was used. Potentials were referred to an Ag/0.01 M $AgNO_3$ reference electrode in MeCN + 0.1 M Bu_4NClO_4 and measured potentials were calibrated through the use of an internal Fc/Fc^+ standard. The working electrode was a vitreous carbon disk (3 mm in diameter) polished with 2 µm diamond paste (Mecaprex Presi; Ep_a, anodic peak potential; Ep_c, cathodic peak potential; $E_{1/2} = (Ep_a + Ep_c)/2$; $\Delta E_p = Ep_a - Ep_c$). The auxiliary electrode was a Pt wire in MeCN + 0.1 M *n*-Bu_4NClO_4 or *n*-Bu_4NCl, or in CH_2Cl_2 + 0.1 M Bu_4NClO_4 solution.

Synthesis of [$Cr^{III}LCl(CH_3CN)$]. A mixture of LH_2 (29 mg L, 50 µmol) and solid NaH (60 % in mineral oil, 16.7 mg, 200 µmol) were stirred for 30 minutes in THF (2 mL) at 293 K. The insoluble material was filtered off, and a suspension of $CrCl_3(THF)_3$ (19 mg, 50 µmol) in THF (2 mL) was added to the resulting solution. The color turned from yellow to purple-red, during which all the powder was dissolved. After a few minutes of reaction, a red precipitate appeared. After 2 hours, the fine powder was isolated by centrifugation. The powder was then redissolved in a CH_2Cl_2:MeOH mixture (90:10) and then filtered to remove the insoluble residue (NaCl). The resulting solution was then concentrated to 0.5 mL, and 1 mL of CH_3CN was added. The color changed from brown to yellow-orange during the process, and a precipitate was formed. The resulting yellow powder was filtered, washed with CH_3CN, and dried, corresponding to [$Cr^{III}LCl(CH_3CN)$] (30.2 mg, 86 %). X-ray suitable [$Cr^{III}LCl(CH_3CN)$] yellow crystals were obtained by diffusion of CH_3CN into a CH_2Cl_2 solution of [$Cr^{III}LCl(CH_3CN)$] at 293 K. ESI-MS (CH_3CN, m/z,): 630.04, $[Cr^{III}L]^+$. IR (cm^{-1}): 2302 (d, CN), 1595 (s), 1565 (s), 1480 (m), 1438 (s), 1267 (w), 1081 (m), 1021 (s), 842(s), 797 (s), 753 (s). λ_{max} in CH_2Cl_2: 431, 523 nm. Anal. Calcd. for $C_{38}H_{30}ClCrN_2S_2 \cdot 0.4CH_3CN \cdot 2H_2O$ (718.69): C, 64.84; H, 4.94; N, 4.68; S, 8.92; Found: C, 64.81; H, 4.59; N, 4.70; S, 9.03.

Synthesis of [$Cr^{III}LCl$]. X-ray suitable red-purple [$Cr^{III}LCl$] crystals were obtained by diffusion of *n*-pentane into a CH_2Cl_2 solution of [$Cr^{III}LCl(CH_3CN)$] at 293 K. IR (cm^{-1}): 1595 (s), 1565 (s), 1479 (d), 1440 (s), 1274 (w), 1029 (m), 790 (s), 738 (s). λ_{max} in CH_3CN: 437, 486 nm. (quantitative yield). ESI-MS (CH_3CN, m/z,): 630.04, $[Cr^{III}L]^+$. Anal. Calcd. for $C_{38}H_{30}ClCrN_2S_2 \cdot C_5H_{12} \cdot 0.7CH_2Cl_2 \cdot 0.5C_4H_{10}O$ (832.99): C, 65.74; H, 5.84; N, 3.36; S, 7.68; Found: C, 65.59; H, 5.66; N, 3.04; S, 7.68.

Synthesis of *n*-$Bu_4N[Cr^{III}LCl_2]$. *n*-Bu_4NCl (2.8 mg, 10 µmol) was added to a CH_2Cl_2 solution (2 mL) of [$Cr^{III}LCl(CH_3CN)$] (7 mg, 10 µmol). The volume was reduced to 0.2 mL, and THF (2 mL) was added. A precipitate corresponding to *n*-$Bu_4N[Cr^{III}LCl_2]$ was formed and collected (9 mg, quantitative yield). X-ray suitable red-orange crystals of $[Cp_2Co][Cr^{III}LCl_2]$ were obtained by diffusing THF into a CH_2Cl_2 solution containing [Cp_2CoCl] (2.3 mg, 10 µmol) and [$Cr^{III}LCl(CH_3CN)$] (7 mg, 10 µmol). ESI-MS (CH_3CN, m/z,): 700.13, $[Cr^{III}LCl_2]^-$. IR (cm^{-1}): 1595 (s), 1569 (s), 1483 (m), 1438 (s), 1273 (w), 1021 (m), 798 (s), 750 (d), 697 (s).

Synthesis of [$Cr^{III}_2L_2(\mu\text{-}Cl)(\mu\text{-}OH)$]. Cp_2Co (3.8 mg, 20 µmol) was added to a THF (2 mL) suspension of [$Cr^{III}LCl(CH_3CN)$] (14 mg, 20 µmol) and stirred overnight. The resulting deep green precipitate was filtered and washed with CH_3CN. The powder was then dissolved in a solution of THF (1 mL) containing 50 µL of water. The solution was then concentrated to dryness under vacuum and the residue redissolved in CH_2Cl_2. X-ray suitable deep yellow crystals were obtained by diffusing THF into the CH_2Cl_2

solution of the product (5.8 mg, 8.8 µmol, 44 %). ESI-MS (CH_3CN, m/z,): 630.04, $[Cr^{III}L]^+$. IR (cm^{-1}): 2915 (m, OH), 1597 (s), 1561 (d), 1485 (s), 1465(m), 1438 (s), 1377(s), 1270 (d), 1055(s), 1023 (m), 971 (s), 831(s), 790 (m), 740 (m), 693 (s), 653 (d). λ_{max} in CH_2Cl_2: 481 nm.

Synthesis of $[Cr^{III}(L^{N2S})_2](BF_4)$. $HBF_4{\cdot}Et_2O$ (3.3 mg, 20 µmol) was added to an CH_3CN suspension (2 mL) of $[Cr^{III}LCl(CH_3CN)]$ (14 mg, 20 µmol). The yellow suspension turned to an orange solution. Cp_2Co (3.8 mg, 20 µmol) was added and the mixture was stirred overnight. The resulting deep green precipitate was filtered and washed with CH_3CN. The powder was then dissolved in an CH_3CN solution (1 mL) containing 50 µL of water. X-ray suitable red crystals were obtained by slow evaporation (3.8 mg, 31 µmol, 29 %). ESI-MS (CH_3CN, m/z,): 1142.35, $[Cr^{III}L^{N2S}{}_2]^+$. IR (cm^{-1}): 1597 (s), 1567 (s), 1466 (d), 1430 (d), 1284 (w), 1165 (d), 1068 (d), 1021 (s), 982 (w), 900 (s), 788 (s), 743 (s), 693 (s), 656 (d).

Detection of H_2S. To an MeCN solution (4 mL) of $[Cr^{III}(LSH)Cl(CH_3CN)]^+$ (250 mM, 1 mmol), 1 equiv. of Cp_2Co (1 mmol) was added in a closed vial under stirring. After 1 hour of reaction, water (50 µL) or 1 equiv. of HBF_4 (1 mmol) was added. The gas phase was then introduced to a MeCN solution (5 mL) of dansyl azide (5 mmol) using the freeze pump-thaw method, and the amount of H_2S was quantified by the fluorescence enhancement (Figure S8).[55]

Synthesis of the 5-(dimethylamino)-1-naphthalenesulfonamide (dansyl azide). The synthetic protocol from the literature[55] was partially modified. To a solution of sodium azide (693.0 mg, 11 mmol, 1.1 eq. dissolved in 30 mL of a 1:1 water/EtOH mixture) a suspension of dansyl chloride (2 g, 10 mmol, 1.0 eq.) in EtOH was added dropwise over the course of 10 minutes. Upon addition, the reaction mixture was stirred at room temperature for 3 hours. The EtOH was removed *in vacuo*, and the yellow aqueous phase was extracted three times using 20 mL portions of DCM. The organic layer was dried over sodium sulfate, and the DCM was removed *in vacuo* without heating. The product was obtained as a yellow crystalline solid (2.1 g, 77%) and used without further purification. ^{1}H NMR (300 MHz, $CDCl_3$) δ: 8.63 (1H, dt), 8.30 (1H, dd), 8.17 (1H, dt), 7.56 (2H, ddd), 7.20 (1H, dd), 2.86 (6H, s). ^{13}C NMR (75 MHz, $CDCl_3$) δ: 152.2, 133.7, 130.1, 130.0, 129.6, 129.3, 123.0, 118.8, 115.8, 45.4.

Acknowledgments

The authors gratefully acknowledge research support of this work by the China Scholarship Council (KS), the French National Agency for Research in the framework of the "Investissements d'avenir" program (ANR-15-IDEX-02), the Labex ARCANE, CBH-EUR-GS (ANR-17-EURE-0003) and the Deutsche Forschungsgemeinschaft (DFG, Me 1313/13-2 and Me1313/14-1, project numbers 311772602 and 316698085, respectively). Purchase of the SQUID magnetometer was enabled by the DFG (INST 186/1329-1 FUGG, project number 423442764) and the Niedersächsische Ministerium für Wissenschaft und Kultur (MWK).

Supporting Information

The Supporting Information is available free of charge at https://pubs.acs.org/doi/xxx.

Crystallographic tables

ESI-mass spectra

Further UV-vis absorption and cyclic voltammetry data (PDF).

Accession Codes

CCDC 2311590-2311594 contain the supplementary crystallographic data for this paper. These data can be obtained free of charge via www.ccdc.cam.ac.uk/data_request/cif, or by emailing data_request@ccdc.cam.ac.uk, or by contacting The Cambridge Crystallographic Data Centre, 12 Union Road, Cambridge CB2 1EZ, UK; fax: +44 1223 336033.

References

1. W. D. Jones, D. A. Vivic, R. Martin Chin, J. H. Roache, A. W. Myers, Homogeneus models of thiophene HDS reactions. Selectivity in thiophene C S cleavage and thiophene reactions with dinuclear metal complexes. *Polyhedron* **1997,** *16*, 3115-3128
2. R. J. Angelici, An overview of modeling studies in HDS, HDN and HDO catalysis. *Polyhedron* **1997,** *16*, 3073-3088
3. C. Bianchini, A. Meli, Hydrogenation, Hydrogenolysis, and Desulfurization of Thiophenes by Soluble Metal Complexes: Recent Achievements and Future Directions. *Acc. Chem. Res.* **1998,** *31*, 109-116
4. S. Brunet, D. Mey, G. Pérot, C. Bouchy, F. Diehl, On the hydrodesulfurization of FCC gasoline: a review. *Appl. Catal. A: Gen.* **2005,** *278*, 143-172
5. T. Ganguly, A. B. Chakraborty, A. Majumdar, Transition Metal Mediated Hydrolysis of C–S Bonds: An Overview of a New Reaction Strategy. *ACS Org. Inorg. Au* **2023**,
6. D. Buccella, K. E. Janak, G. Parkin, Reactivity of Mo(PMe3)6 towards Benzothiophene and Selenophenes: New Pathways Relevant to Hydrodesulfurization. *J. Am. Chem. Soc.* **2008,** *130*, 16187-16189
7. Z. Wang, Y. Kuninobu, M. Kanai, Molybdenum-Mediated Desulfurization of Thiols and Disulfides. *Synlett* **2014,** *25*, 1869-1872
8. X.-F. Gao, J.-J. Du, Z. Liu, J. Guo, Visible-Light-Induced Specific Desulfurization of Cysteinyl Peptide and Glycopeptide in Aqueous Solution. *Org. Lett.* **2016,** *18*, 1166-1169
9. A. K. Singh, R. Mukherjee, Cobalt(ii) and cobalt(iii) complexes of thioether-containing hexadentate pyrazine amide ligands: C–S bond cleavage and cyclometallation reaction. *Dalton Trans.* **2008**, 260-270
10. N. H. Chan, J. H. Roache, W. D. Jones, Carbon–sulfur bond cleavage of benzothiophene by Cp∗Co(C2H4)2. *Inorg. Chim. Acta* **2015,** *437*, 36-40
11. M. Hirotsu, K. Santo, H. Hashimoto, I. Kinoshita, Carbon- and Sulfur-Bridged Diiron Carbonyl Complexes Containing N,C,S-Tridentate Ligands Derived from Functionalized Dibenzothiophenes: Mimics of the [FeFe]-Hydrogenase Active Site. *Organometallics* **2012,** *31*, 7548-7557
12. K. Pramanik, U. Das, B. Adhikari, D. Chopra, H. Stoeckli-Evans, RhCl3-Assisted C−H and C−S Bond Scissions: Isomeric Self-Association of Organorhodium(III) Thiolato Complex. Synthesis, Structure, and Electrochemistry. *Inorg. Chem.* **2008,** *47*, 429-438
13. M. Shibue, M. Hirotsu, T. Nishioka, I. Kinoshita, Ruthenium and Rhodium Complexes with Thiolate-Containing Pincer Ligands Produced by C−S Bond Cleavage of Pyridyl-Substituted Dibenzothiophenes. *Organometallics* **2008,** *27*, 4475-4483
14. M. Jana, A. Majumdar, C–S Bond Cleavage, Redox Reactions, and Dioxygen Activation by Nonheme Dicobalt(II) Complexes. *Inorg. Chem.* **2018,** *57*, 617-632
15. N. Pal, A. Majumdar, Transfer of hydrosulfide from thiols to iron(ii): a convenient synthetic route to nonheme diiron(ii)–hydrosulfide complexes. *Dalton Trans.* **2019,** *48*, 5903-5908
16. T. Ganguly, A. Majumdar, Comparative Study for the Cobalt(II)- and Iron(II)-Mediated Desulfurization of Disulfides Demonstrating That the C–S Bond Cleavage Step Precedes the S–S Bond Cleavage Step. *Inorg. Chem.* **2020,** *59*, 4037-4048
17. D. G. Churchill, B. M. Bridgewater, G. Parkin, Modeling Aspects of Hydrodesulfurization at Molybdenum: Carbon−Sulfur Bond Cleavage of Thiophenes by Ansa Molybdenocene Complexes. *J. Am. Chem. Soc.* **2000,** *122*, 178-179

18. B. Kumar Santra, G. Kumar Lahiri, Ruthenium-, osmium- and cobalt-ion mediated selective activation of a C–Cl bond. Direct and spontaneous aromatic thiolation reaction via C–S bond cleavage. *J. Chem. Soc. Dalton Trans.* **1998**, 1613-1618
19. K. Osakada, H. Hayashi, M. Maeda, T. Yamamoto, A. Yamamoto, PREPARATION AND PROPERTIES OF NEW THIOLATO- AND MERCAPTO-TRANSITION METAL COMPLEXES, MR(SR′)(PR″3)2 (M = Ni, Pd; R = H, Ar; R′ = H, Ar). EVOLUTION OF R–R′ FROM THE COMPLEXES THROUGH CLEAVAGE OF THE S–R′ BOND. *Chem. Lett.* **2006,** *15*, 597-600
20. T. Ganguly, A. Bera, A. B. Chakraborty, A. Majumdar, Catalytic Hydrolysis of Thiolates to Alcohols. *Inorg. Chem.* **2022,** *61*, 7377-7386
21. J. Torres-Nieto, A. Arévalo, J. J. García, Catalytic Desulfurization of Dibenzothiophene and Its Hindered Analogues with Nickel and Platinum Compounds. *Organometallics* **2007,** *26*, 2228-2233
22. N. Barbero, R. Martin, Ligand-Free Ni-Catalyzed Reductive Cleavage of Inert Carbon–Sulfur Bonds. *Org. Lett.* **2012,** *14*, 796-799
23. K. Yamada, T. Yanagi, H. Yorimitsu, Generation of Organozinc Reagents from Arylsulfonium Salts Using a Nickel Catalyst and Zinc Dust. *Org. Lett.* **2020,** *22*, 9712-9718
24. M. Lee, S. Neukirchen, C. Cabrele, O. Reiser, Visible-light photoredox-catalyzed desulfurization of thiol- and disulfide-containing amino acids and small peptides. *J. Pept. Sci.* **2017,** *23*, 556-562
25. A. Sattler, G. Parkin, Carbon−Sulfur Bond Cleavage and Hydrodesulfurization of Thiophenes by Tungsten. *J. Am. Chem. Soc.* **2011,** *133*, 3748-3751
26. M. A. Kopf, D. Varech, J. P. Tuchagues, D. Mansuy, I. Artaud, New intermediate-spin chloroiron(III) complex with a mixed nitrogen-sulfur co-ordination. *J. Chem. Soc. Dalton Trans.* **1998**, 991-998
27. M. Gennari, C. Duboc, Bio-inspired, Multifunctional Metal-Thiolate Motif: From Electron Transfer to Sulfur Reactivity and Small-Molecule Activation. *Acc. Chem. Res.* **2020,** *53*, 2753-2761
28. A. C. Ghosh, C. Duboc, M. Gennari, Synergy between metals for small molecule activation: Enzymes and bio-inspired complexes. *Coord. Chem. Rev.* **2021,** *428*,
29. M. Gennari, M. Orio, J. Pécaut, F. Neese, M.-N. Collomb, C. Duboc, Reversible Apical Coordination of Imidazole between the Ni(III) and Ni(II) Oxidation States of a Dithiolate Complex: A Process Related to the Ni Superoxide Dismutase. *Inorg. Chem.* **2010,** *49*, 6399-6401
30. D. Brazzolotto, M. Gennari, S. Yu, J. Pécaut, M. Rouzières, R. Clérac, M. Orio, C. Duboc, An Experimental and Theoretical Investigation on Pentacoordinated Cobalt(III) Complexes with an Intermediate S=1 Spin State: How Halide Ligands Affect their Magnetic Anisotropy. *Chem. Eur. J.* **2016,** *22*, 925-933
31. L. K. Wang, M. Zlatar, F. Vlahovic, S. Demeshko, C. Philouze, F. Molton, M. Gennari, F. Meyer, C. Duboc, M. Gruden, Experimental and Theoretical Identification of the Origin of Magnetic Anisotropy in Intermediate Spin Iron(III) Complexes. *Chem. Eur. J.* **2018,** *24*, 5091-5094
32. M. Gennari, D. Brazzolotto, S. Yu, J. Pecaut, C. Philouze, M. Rouzieres, R. Clerac, M. Orio, C. Duboc, Effect of the Metal on Disulfide/Thiolate Interconversion: Manganese versus Cobalt. *Chem. Eur. J.* **2015,** *21*, 18770-18778
33. A. W. Addison, T. N. Rao, J. Reedijk, J. Vanrijn, G. C. Verschoor, SYNTHESIS, STRUCTURE, AND SPECTROSCOPIC PROPERTIES OF COPPER(II) COMPOUNDS CONTAINING NITROGEN SULFUR DONOR LIGANDS - THE CRYSTAL AND MOLECULAR-STRUCTURE OF AQUA 1,7-BIS(N-METHYLBENZIMIDAZOL-2'-YL)-2,6-DITHIAHEPTANE COPPER(II) PERCHLORATE. *J. Chem. Soc. Dalton Trans.* **1984**, 1349-1356
34. A. G. Blackman, E. B. Schenk, R. E. Jelley, E. H. Krenske, L. R. Gahan, Five-coordinate transition metal complexes and the value of τ5: observations and caveats. *Dalton Trans.* **2020,** *49*, 14798-14806
35. M. Gennari, M. Orio, J. Pécaut, E. Bothe, F. Neese, M.-N. Collomb, C. Duboc, Influence of Mixed Thiolate/Thioether versus Dithiolate Coordination on the Accessibility of the Uncommon +I and +III Oxidation States for the Nickel Ion: An Experimental and Computational Study. *Inorg. Chem.* **2011,** *50*, 3707-3716

36. D. Brazzolotto, M. Gennari, N. Queyriaux, T. R. Simmons, J. Pécaut, S. Demeshko, F. Meyer, M. Orio, V. Artero, C. Duboc, Nickel-centred proton reduction catalysis in a model of [NiFe] hydrogenase. *Nat. Chem.* **2016,** *8*, 1054–1060
37. L. Wang, M. Gennari, A. Barrozo, J. Fize, C. Philouze, S. Demeshko, F. Meyer, M. Orio, V. Artero, C. Duboc, Role of the Metal Ion in Bio-Inspired Hydrogenase Models: Investigation of a Homodinuclear FeFe Complex vs Its Heterodinuclear NiFe Analogue. *ACS Catal.* **2020**, 177-186
38. B. Hwang, M.-S. Park, K. Kim, Ferrocene and Cobaltocene Derivatives for Non-Aqueous Redox Flow Batteries. *ChemSusChem* **2015,** *8*, 310-314
39. S. Schäfer, J. Becker, A. Beitat, C. Würtele, Investigation of Chromium Complexes with a Series of Tripodal Ligands. *Z. Anorg. Allg. Chem.* **2013,** *639*, 2269-2275
40. N. J. Robertson, M. J. Carney, J. A. Halfen, Chromium(II) and Chromium(III) Complexes Supported by Tris(2-pyridylmethyl)amine: Synthesis, Structures, and Reactivity. *Inorg. Chem.* **2003,** *42*, 6876-6885
41. D. J. Hodgson, M. H. Zietlow, E. Pedersen, H. Toftlund, Synthesis and magnetic and structural characterization of the binuclear complex di-μ-hydroxobis{[tris(2-pyridylmethyl)amine]chromium(III)} perchlorate tetrahydrate, [(tpa)CrOH]2(ClO4)4·4H2O. *Inorg. Chim. Acta* **1988,** *149*, 111-117
42. B. G. Gafford, R. A. Holwerda, Oxidative synthesis of bis(.mu.-hydroxo)chromium(III) dimers with aromatic amine ligands. Structure, physical properties, and base hydrolysis kinetics of the bis(.mu.-hydroxo)bis[(tris(2-pyridylmethyl)amine)chromium(III)] ion. *Inorg. Chem.* **1989,** *28*, 60-66
43. A. E. Ceniceros-Gómez, N. Barba-Behrens, M. E. Quiroz-Castro, S. Bernès, H. Nöth, S. E. Castillo-Blum, Synthesis, X-ray and spectroscopic characterisation of chromium(III) coordination compounds with benzimidazolic ligands. *Polyhedron* **2000,** *19*, 1821-1827
44. D. Brazzolotto, F. G. Cantú Reinhard, J. Smith-Jones, M. Retegan, L. Amidani, A. S. Faponle, K. Ray, C. Philouze, S. P. de Visser, M. Gennari, C. Duboc, A High-Valent Non-Heme μ-Oxo Manganese(IV) Dimer Generated from a Thiolate-Bound Manganese(II) Complex and Dioxygen. *Angew. Chem. Int. Ed.* **2017,** *56*, 8211-8215
45. M. Gennari, D. Brazzolotto, J. Pecaut, M. V. Cherrier, C. J. Pollock, S. DeBeer, M. Retegan, D. A. Pantazis, F. Neese, M. Rouzieres, R. Clerac, C. Duboc, Dioxygen Activation and Catalytic Reduction to Hydrogen Peroxide by a Thiolate-Bridged Dimanganese(II) Complex with a Pendant Thiol. *J. Am. Chem. Soc.* **2015,** *137*, 8644-8653
46. L. K. Wang, M. Gennari, F. G. C. Reinhard, S. K. Padamati, C. Philouze, D. Flot, S. Demeshko, W. R. Browne, F. Meyer, S. P. de Visser, C. Duboc, O-2 Activation by Non-Heme Thiolate-Based Dinuclear Fe Complexes. *Inorg. Chem.* **2020,** *59*, 3249-3259
47. K. Izutsu, *Acid-Base Dissociation Constants in Dipolar Aprotic Solvents*. Blackwell Scientific: Oxford, U.K. , 1990.
48. J. L. Dempsey, B. S. Brunschwig, J. R. Winkler, H. B. Gray, Hydrogen Evolution Catalyzed by Cobaloximes. *Acc. Chem. Res.* **2009,** *42*, 1995-2004
49. K. Yang, Q. Li, Z. Li, X. Sun, Transition-metal-free C–S bond cleavage and transformation of organosulfur compounds. *Chem. Commun.* **2023,** *59*, 5343-5364
50. M. S. Akhlaq, C. Von Sonntag, Free-radical-induced elimination of hydrogen sulfide from dithiothreitol. A chain reaction. *J. Am. Chem. Soc.* **1986,** *108*, 3542-3544
51. T.-Y. Luh, Z.-J. Ni, Transition-Metal-Mediated C-S Bond Cleavage Reactions. *Synthesis* **1990,** *1990*, 89-103
52. Y. Hebting, P. Adam, P. Albrecht, Reductive Desulfurization of Allylic Thiols by HS-/H2S in Water Gives Clue to Chemical Reactions Widespread in Natural Environments. *Org. Lett.* **2003,** *5*, 1571-1574
53. M. J. Chalkley, P. H. Oyala, J. C. Peters, Cp* Noninnocence Leads to a Remarkably Weak C–H Bond via Metallocene Protonation. *J. Am. Chem. Soc.* **2019,** *141*, 4721-4729
54. Wade C. Henke, Y. Peng, Alex A. Meier, E. Fujita, David C. Grills, Dmitry E. Polyansky, James D. Blakemore, Mechanistic roles of metal- and ligand-protonated species in hydrogen evolution with [Cp*Rh] complexes. *PNAS* **2023,** *120*, e2217189120

55. H. Peng, Y. Cheng, C. Dai, A. L. King, B. L. Predmore, D. J. Lefer, B. Wang, A Fluorescent Probe for Fast and Quantitative Detection of Hydrogen Sulfide in Blood. *Angew. Chem. Int. Ed.* **2011,** *50*, 9672-9675
56. M. Gennari, J. Pécaut, M. N. Collomb, C. Duboc, A Copper Thiolate Centre for Electron Transfer: Mononuclear versus Dinuclear Complexes. *Dalton Trans.* **2012,** *41*, 3130-3133
57. M. Gennari, M. Retegan, S. DeBeer, J. Pecaut, F. Neese, M. N. Collomb, C. Duboc, Experimental and Computational Investigation of Thiolate Alkylation in Ni-II and Zn-II Complexes: Role of the Metal on the Sulfur Nucleophilicity. *Inorg. Chem.* **2011,** *50*, 10047-10055
58. M. Gennari, B. Gerey, N. Hall, J. Pécaut, H. Vezin, M. N. Collomb, M. Orio, C. Duboc, Structural, spectroscopic and redox properties of a mononuclear Co-II thiolate complex - the reactivity toward S-alkylation: an experimental and theoretical study. *Dalton Trans.* **2012,** *41*, 12586-12594
59. L. Wang, M. Gennari, F. G. Cantú Reinhard, J. Gutiérrez, A. Morozan, C. Philouze, S. Demeshko, V. Artero, F. Meyer, S. P. de Visser, C. Duboc, A Non-Heme Diiron Complex for (Electro)catalytic Reduction of Dioxygen: Tuning the Selectivity through Electron Delivery. *J. Am. Chem. Soc.* **2019,** *141*, 8244-8253
60. S. L. Hooe, J. M. Dressel, D. A. Dickie, C. W. Machan, Highly Efficient Electrocatalytic Reduction of CO2 to CO by a Molecular Chromium Complex. *ACS Catal.* **2020,** *10*, 1146-1151
61. G. M. Sheldrick SHELXTL-Plus, Structure Determination Software Programs, (Version 6.14.), Bruker Analytical X-ray Instruments Inc., Madison, Wisconsin, USA, 1998.

For Table of Contents Only

A series of bis-thiolate Cr^{III} complexes is described. Unexpectedly with this N2S2 ligand, the mononuclear compounds can arrange a 6-coordination mode around the Cr ion. Besides, $[Cr^{III}LCl(CH_3CN)]$ display desulfurization reactivity under reducing conditions leading to a mononuclear Cr^{III} complex bearing two ligands in which one thiolate function has been removed.